Molecular Biology of the Cell
Vol. 17, 475–484, January 2006

Essential Roles in Development and Pigmentation for the *Drosophila* Copper Transporter DmATP7[D] [V]

Melanie Norgate,*† Esther Lee,*† Adam Southon,* Ashley Farlow,*† Philip Batterham,*† James Camakaris,* and Richard Burke*

*Department of Genetics and †Centre for Environmental Stress and Adaptation Research, The University of Melbourne, Parkville VIC 3010, Australia

Submitted June 6, 2005; Revised September 29, 2005; Accepted October 17, 2005
Monitoring Editor: Jeffrey Brodsky

Defects in the mammalian Menkes and Wilson copper transporting P-type ATPases cause severe copper homeostasis disease phenotypes in humans. Here, we find that *DmATP7*, the sole *Drosophila* orthologue of the *Menkes* and *Wilson* genes, is vital for uptake of copper in vivo. Analysis of a *DmATP7* loss-of-function allele shows that *DmATP7* is essential in embryogenesis, early larval development, and adult pigmentation and is probably required for copper uptake from the diet. These phenotypes are analogous to those caused by mutation in the mouse and human *Menkes* genes, suggesting that like Menkes, *DmATP7* plays at least two roles at the cellular level: delivering copper to cuproenzymes required for pigmentation and neuronal function and removing excess cellular copper via facilitated efflux. *DmATP7* displays a dynamic and unexpected expression pattern in the developing embryo, implying novel functions for this copper pump and the lethality observed in *DmATP7* mutant flies is the earliest seen for any copper homeostasis gene.

INTRODUCTION

Copper is a trace element essential for all aerobic organisms. It is required by copper-dependent enzymes involved in diverse metabolic processes, including cellular respiration, antioxidant defense, pigment formation, neurotransmitter production, and peptide biosynthesis (Danks, 1988). However, the redox potential that makes copper such an effective cofactor also makes it extremely toxic if levels are not properly controlled, a property that has resulted in tightly regulated homeostatic mechanisms, well conserved from yeast to humans (Halliwell and Gutteridge, 1984; Pena *et al*., 1999). A key aspect of metal homeostasis is regulated export, or efflux, of the metal from individual cells. In single-celled organisms such as yeast, metal export serves mainly a detoxification role. In a multicellular organism, however, essential metals such as copper that are absorbed from dietary sources must be distributed to different tissues throughout the body. Therefore, export of copper from individual cells is necessary both for detoxification and for systemic supply.

The primary human copper exporters are the Menkes and Wilson copper-transporting P-type ATPases. These proteins show 54% sequence identity and at the cellular level function in a similar way to transport copper across membranes (Lutsenko and Petris, 2002). However, the human diseases associated with disruption of their respective functions are very different and illustrate the dual nature of copper. Menkes disease is an X-linked recessive disorder that presents as a severe systemic copper deficiency with symptoms including growth failure, skeletal defects, and progressive degeneration of the central nervous system, resulting in death during early childhood (Danks, 1995). The Menkes disease protein MNK (or ATP7A) is expressed in all tissues except the liver and is thought to play two roles at the cellular level: at basal or low intracellular copper levels, it delivers copper to enzymes of the secretory pathway in the *trans*-Golgi network (TGN) (Yamaguchi *et al*., 1996; Petris *et al*., 2000); and at high intracellular copper concentrations, MNK translocates to the plasma membrane where it catalyzes copper efflux (Petris *et al*., 1996). MNK is expressed in the mucosal cells lining the intestine and is required in these cells for systemic absorption of copper. In patients with Menkes disease, copper is trapped in the intestinal mucosa and very little is delivered to peripheral organs and tissues (Danks *et al*., 1972). In contrast, Wilson disease is caused by accumulation of copper in the liver and brain, leading to chronic liver disease, cirrhosis, and neurological problems such as behavioral disturbances and movement disorders (Scheinberg and Sternlieb, 1984). The protein involved is WND (or ATP7B), and it is expressed mainly in the liver and delivers copper to apoceruloplasmin in the *trans*-Golgi network. At elevated copper levels, WND traffics to the biliary canalicular membrane where copper is incorporated into the bile for excretion from the body (Roelofsen *et al*., 2000). The failure of this copper excretion function in Wilson disease patients leads to toxic copper accumulation.

In both cases described above, disruption of copper transport causes serious disease, although the phenotypes are effectively opposite, and normally MNK and WND function in complementary tissues and together maintain copper homeostasis. Although mammals have two copper-translocating P-type ATPases performing complementary functions,

This article was published online ahead of print in *MBC in Press* (http://www.molbiolcell.org/cgi/doi/10.1091/mbc.E05–06–0492) on October 26, 2005.

[D] [V] The online version of this article contains supplemental material at *MBC Online* (http://www.molbiolcell.org).

Address correspondence to: James Camakaris (j.camakaris@unimelb.edu.au).

Abbreviations used: AEL, after egg laying; BCS, bathocuproinedisulfonic acid; PM, plasma membrane; TGN, *trans*-Golgi network; TTM, tetrathiomolybdate.

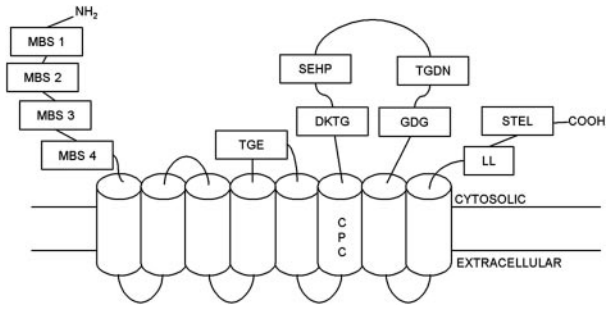

Figure 1. Schematic diagram of DmATP7 based on the predicted MNK structure. The N-terminal domain comprises four GMxCxxC metal binding sites (MBS1–4; mammalian MNK and WND have six). The conserved cation transduction motif CPC lies in the sixth of eight transmembrane domains. The CPC motif and proposed ATP-binding site SEHP are conserved in transition metal transporting P-type ATPases. ATP hydrolysis requires the TGE, DKTG, TGDN, and GDGVNDSP (labeled GDG) sites characteristic of all P-type ATPases (identical to MNK/WND except MNK has GDGINDSP sequence). The C-terminal dileucine motif (LL; WND has three leucines at this location) is required for endocytosis and basolateral targeting, and STEL (DTAL in MNK) is a putative PDZ target motif required for localization to the basolateral membrane of polarized cells. A sequence alignment between MNK, WND, and DmATP7 is available in Supplemental Material 1.

lower multicellular animals such as insects (*Drosophila melanogaster* and *Anopheles gambiae*) and nematodes (*Caenorhabditis elegans*) have only one, raising the question as to whether this sole copper pump fulfills some or all of the functions of its mammalian orthologues. To better understand the function and regulation of these vital copper-transporting P-type ATPases, this study sought to characterize the in vivo role of the sole *Drosophila* orthologue, *DmATP7*. We had previously identified *DmATP7* as an X-linked *Drosophila* gene predicted to encode a protein with strong homology to both MNK and WND. Importantly, all motifs shown to be essential for copper transport in the mammalian P-type ATPases are highly conserved in *DmATP7* (Figure 1). Knockdown of the *DmATP7* transcript in cultured *Drosophila* embryonic "S2" cells by RNA interference resulted in a significant increase in copper accumulation within these cells, confirming a role for *DmATP7* in copper efflux analogous to that seen in other systems (Southon *et al*., 2004).

This work investigates *DmATP7* function in *Drosophila*, generating a loss-of-function *DmATP7* mutant allele to analyze its role in embryogenesis, early larval development, and adult pigmentation formation. The embryonic *DmATP7* expression pattern and localization of the DmATP7 protein in larval tissues is also examined, and the importance of key conserved residues is investigated in an in vivo overexpression assay. Our results reveal several vital functions for *DmATP7* and establish *Drosophila* as an excellent animal model for investigating the regulation of these essential copper efflux pumps.

MATERIALS AND METHODS

Fly Stock Maintenance and Media

Fly stocks were maintained and experiments were performed at 25°C on standard laboratory medium, supplemented with either 100 μM bathocuproinedisulfonic acid (BCS; Sigma-Aldrich, St. Louis, MO) to make copper-deficient food medium, or 1 mM copper ($CuSO_4 \cdot 5H_2O$; Merck, Whitehouse Station, NJ) to make copper-supplemented medium. Tetrathiomolybdate (TTM; Sigma-Aldrich) was used instead of BCS where indicated in figure legends. In the add-back experiments presented in Table 1, 50 μM BCS media was supplemented with either 50 μM copper, 200 μM zinc ($ZnSO_4$-$7H_2O$; Ajax Finechem, Seven Hills, Australia), or 100 μM iron ($FeSO_4 \cdot 7H_2O$; BDH, Poole, Dorset, United Kingdom).

Generation of DmATP7 Null Allele

A *DmATP7* null allele (ΔP17) was generated using imprecise excision of a single P-element inserted ~340 base pairs upstream of the *DmATP7* transcription start site in the EP308 line (*w^{1118} P{w^+ = EP}ATP7^{EP308}*; BL10114, Bloomington Stock Center, Indiana University, Bloomington, IN). To mobilize the P-element, EP308 flies were crossed to a line containing a stable transposase source (*Sb^1 P{Delta2-3}99B/TM6B*; BL1798; Bloomington Stock Center; Robertson *et al*., 1988), and F1 males containing both the insertion and the transposase source were then crossed to *Binsinscy* females. Finally, single *w^- Sb^+* F2 females that had lost both the transposase source and the P-element were crossed to *Binsinscy* males to establish individual lines. Southern blot analysis followed by sequencing of a PCR product from a hemizygous lethal line identified a 1134-base pair deletion beginning at the EP308 insertion site that removed the transcription start site and the first three metal binding sites of the putative *DmATP7* product, and real-time PCR confirmed loss of expression from *DmATP7*, whereas neighboring genes were unaffected (our unpublished data). This line was subsequently crossed to an *FM7-GFP* line for mutant analysis.

Germline and Somatic Clone Generation

To create embryos lacking maternal *DmATP7* activity, *DmATP7$^{\Delta P17}$ P{FRT(whs)}101/w* ovoD1 v24 P{FRT(whs)}101; P{hsFLP}38* females (ΔP17 is the *DmATP7* loss of function allele described above) were heat shocked for 2 h at 37°C over three consecutive days during larval or pupal development. Adult females were then mated to *FM7-GFP/Y* males. Paternally rescued embryos were detected using the *FM7-GFP* chromosome. To generate adult mosaic flies containing *DmATP7$^{\Delta P17/\Delta P17}$* clones, *DmATP7$^{\Delta P17}$ P{FRT(whs)}101/y1 w67c23 P{Ubi-GFP}ID-1 P{FRT(whs)}101; MKRS, P{hsFLP}86E/+* flies were heat shocked for 2 h at 37°C once during larval development.

Table 1. Rescue of *DmATP7* overexpression-induced hypopigmentation by copper supplementation

	Cu (mM)		TTM (μM)			BCS (μM)					BCS (50 μM) + supplement		
	1–3	NF	2.5	5	10	5	10	20	50	100	Cu	Zn	Fe
DmATP7 overexpression	+	+	1	2	3	+	+	1	2	3	+	2	2
Wild type	+	+	+	+	+	+	+	+	+	+	−	−	−

Abdominal pigmentation levels of *DmATP7* overexpression (*Act-GAL4; EP lineGS6038*) and wild-type (*Act-GAL4; +*) adults raised on media indicated: + is wild-type pigmentation, and 1, 2, and 3 represent mild, moderate, and extreme hypopigmentation, respectively. Wild type was not screened on supplemented BCS media (−). NF is normal food media. Hypopigmentation is visible only in flies raised on copper-deficient media (TTM or BCS) and is rescued by addition of copper back into the media, but not addition of zinc or iron, indicating it is caused specifically by copper deficiency. The degree of hypopigmentation is proportional to the amount of chelator in the media; therefore, pigmentation is sensitive to the amount of available copper.

Overexpression Fly Strains and Transgenics

GAL4 lines used were as follows: *Pnr-GAL4/Sb*, *Ser* (gift from E. Hafen, University of Zurich, Zurich, Switzerland); *Act-GAL4*; *Tra-GAL4* (gift from P. Whitington, University of Melbourne, Melbourne, Australia); *Ptc-GAL4 w*; P{GawB}ptc559.1* (BL2017; Bloomington Stock Center); GutSpecifc-GAL4 (P. Daborn, University of Melbourne, unpublished data); *w* ovoD1 v24 P{FRT(whs)}101/C(1)DX, y1 f1/Y; P{hsFLP}38* (BL1813; Bloomington Stock Center); *y1 w67c23 P{Ubi-GFP}ID-1 P{FRT(whs)}101* (BL5153; Bloomington Stock Center); *w1118; MKRS, P{hsFLP}86E/TM6B, Tb1* (BL279; Bloomington Stock Center). *MtnA5′-EYFP* and *Ctr1B5′-EYFP* lines were a kind gift from W. Schaffner (University of Zurich). UAS lines generated were *UAS-DmATP7* (CG1886), *UAS-Ctr1A* (CG3977), *UAS-DmCCS* (CG17753), and *UAS-DmAtox1* (CG32446). In addition to the direct *UAS-DmATP7* constructs generated here, an EP line from the Gene Search project (GS6038) was also used to overexpress *DmATP7* from the endogenous locus. This line was used for the experiments in Table 1 and Figure 8B and caused considerably weaker overexpression phenotypes than the direct UAS constructs generated. Full-length cDNAs lacking the C-terminal STOP codon (according to FlyBase annotation; The FlyBase Consortium, 2003; http://flybase.org/) were generated for each gene by PCR amplification from S2 cell-derived cDNA using the following primer pairs (restriction site linkers in uppercase): *DmATP7*, F1 5′ gaGGTACCatgtccacggtgcgcctgcc 3′ and R1 5′ gcTCTAGAcagcttttgcagttcggtAct 3′; *Ctr1A* F1 5′ gaGGTACCatgcaccacgatcacagcg 3′ and R1 5′gcTCTAGAgtgacagtgctcggttacg 3′; *DmCCS* F1 5′ gcGGTACCatgagctccattaagatcgaat 3′ and R1 5′gcTCTAGAcagcttttgtgagcggtcct 3′; and *DmAtox1* F1 5′ gaGGTACCatgacagtgcacgaattcaag 3′ and R1 5′ gcTCTAGAtttcttcaccccgacgtagg 3′.

These full-length cDNAs were cloned into pUAST modified to contain an in-frame C-terminal FLAG epitope tag (MDYKDDDDKA). These pUAST constructs were injected into w^{1118} embryos and transformants selected on the basis of nonwhite eye color. *DmATP7* primers were based on the FlyBase 2002 annotation, and the coding sequence has subsequently been updated and extended 10 aa 5′ to include MPSDERVEAT, lacking in the cDNA used here. In addition, sequencing this PCR product revealed an additional 105 base pairs between base pairs 2634 and base pairs 2635 of CG1886 (GTA CGC AAG TCC ATG GAG CTG AAC AAT CAG CAG TTG CTA TCC GAC TTG GTA TTG GAA CCG GAG GAA GAG CTC CTT ACG GAT CAG AAA ATC ATC GAT TCA CC CGA G) to be exonic sequence, rather than intronic as in the current FlyBase-NG annotation.

Generation of Mutated DmATP7

Wild-type *DmATP7* cDNA was altered using the Transformer site-directed mutagenesis kit (BD Biosciences Clontech, Palo Alto, CA). Oligonucleotides used for mutagenesis are as follows, with altered bases in uppercase. The altered amino acids have been included in parentheses (numbering based on CG1886 FlyBase-NG annotation, November 2004): MBS1, gtgggcatgacttCccagtcgtCtgtgcgcaatatc (C23-S; C26-S), MBS2, gggcatgacctCccagtcgtCcgtgcgcaacatc (C104-S; C107-S); MBS3, ggcatgacgtCcgccagctCtgtggccgcc (C219-S; C222-S); MBS4, gggcatgacttCcgcctcctCcgtcaacaag (C295-S; C298-S); CPC, ggccattgcgGCtccaGCtgctttgggc (C702-A; C704-A); and TAP, ctgtggtcttcgCcaagaccggcac (D746-A).

All mutant *DmATP7* versions were confirmed by sequencing. Only $DmATP7^{MBS}$ was not completely as expected, with the C298 (MBS4) remaining unmutated. These mutant *DmATP7* versions were subcloned into pUAST and used to create transgenic transformants as described above.

Immunohistochemistry, Microscopy, and Western Blotting

Wild-type (w^{1118} or *FM7-GFP*) and *DmATP7* $^{-}$*/Y* embryos were staged, dechorionated in 50% sodium hypochlorite (Ajax Finechem), and fixed for 30 min in 1:1 (vol/vol) heptane (Merck) and 8% paraformaldehyde (PFA; Sigma-Aldrich). The vitelline membrane was removed by shaking in 1:1 methanol (Ajax Finechem): Phosphate-buffered saline (PBS) (Oxoid, Basingstoke, Hampshire, England), and then embryos were rehydrated in PBS. Third instars were dissected and then fixed 30 min in 8% PFA. Primary antibodies used were polyclonal rabbit anti-ATP7a raised against a region of human ATP7a cDNA coding for the six metal-binding sites (used at 1:200; Camakaris *et al*., 1995), monoclonal mouse anti-FLAG (KM5–1C7, used at 1:200; Walter and Eliza Hall Institute Biotechnology Centre, Melbourne, Australia), and monoclonal mouse anti-green fluorescent protein (GFP; used at 1:200). Secondary antibodies from the Alexa Fluor range of IgG-fluorophore conjugates (Invitrogen, Carlsbad, CA) were used to detect primary antibodies. Larval tissue images were recorded with a Zeiss Axioplan 2 fluorescence microscope attached to a Bio-Rad μRadiance control unit using LaserSharp2000 software. Embryonic images were recorded on a Zeiss microscope. Adult *Drosophila* were photographed with an Olympus digital camera through a Leica MZ16 stereomicroscope. Samples for Western blotting were prepared by homogenizing 30 adult fly heads in 60 μl of 2% SDS sample buffer and then lysing on ice for 1 h before clearing lysate by centrifugation. The equivalent of approximately eight fly heads per sample was run on NuPAGE 4–12% Bis-Tris gels (Invitrogen) before transfer to nitrocellulose membranes and Western blotting with monoclonal mouse anti-FLAG primary and polyclonal rabbit anti-mouse horseradish peroxidase-coupled secondary (DakoCytomation, Ely, Cambridgeshire, United Kingdom) antibodies.

Gene Expression Analysis

Wild-type and *DmATP7* $^{-}$*/Y* first instars were transferred within 4 h of hatching to copper-deficient, copper-supplemented, or normal food media for 24 h and then snap frozen in liquid nitrogen. Third instars were transferred to copper-deficient, copper-supplemented, or normal food media for 24 h before dissection in Ringer's solution and transferal of gut and fat bodies to TRIzol (Invitrogen). Total RNA was extracted using the RNeasy kit, including DNase treatment, according to the manufacturer's instructions (QIAGEN, Valencia, CA). cDNA was transcribed from 1 μg of total RNA using avian myeloblastosis virus reverse transcriptase in a 20-μl reaction according to the manufacturer's instructions (Promega, Madison, WI). Primers for real-time PCR were designed using Primer3 software (Rozen and Skaletsky, 2000) available at http://www.broad.mit.edu/genome_software/other/primer3.html. *DmATP7* forward and reverse primers were CCCACTGACCTTCTTCGATACand GGTCTTTCCCTTGGCTATGTrespectively. Other primers have been described previously (Southon *et al*., 2004). Real-time PCR was performed using the Rotor Gene 3000 (Corbett Research, Mortlake, NSW, Australia). Twenty nanograms of reverse transcribed total RNA was amplified in a 25-μl reaction containing 1 μM of each primer and 12.5 μl of 2× QuantiTect SYBR Green PCR Master Mix (QIAGEN). The amount of gene product in each sample was determined using the comparative quantitation method used by the Rotor Gene 5.0 software (Corbett Research) and normalized to *Actin42A* as described previously (Southon *et al*., 2004).

Statistical Analysis

Statistical analysis was conducted using SPSS version 11 (SPSS, Chicago, IL). A one-sample Kolomogorov–Smirinov test was used to assess whether data were normally distributed. Statistical analyses are described in figure legends. Phosphate-buffered saline <0.05 was deemed statistically significant.

RESULTS

DmATP7 Exhibits a Dynamic Expression Pattern during D. melanogaster Embryonic Development

To determine the embryonic expression pattern of *DmATP7*, an anti-MNK antibody that cross-reacts specifically with DmATP7 was used to probe staged *Drosophila* embryos (Figure 2). Although no staining is observed either in *DmATP7* mutant embryos (Figure 2A; see next section) or with preimmune serum (our unpublished data), clear DmATP7 expression is visible at the plasma membrane (PM) of all cells in early embryogenesis (Figure 2E), becoming brighter and taking on a punctate appearance from 2 to 4 h after egg laying (AEL; Figure 2F). From 4 h AEL, the PM staining is replaced by a diffuse cytoplasmic staining. At this time, expression is also seen in early tracheal placodes (Figure 2, C and G), at the edge of the tracheal pit. Expression is then observed in developing tracheae, starting in the trunk (Figure 2H) and extending into the tracheal branches as they develop (Figure 2, I and J). The lack of staining in *DmATP7* mutant embryos or with preimmune serum and the early tracheal staining before tube formation demonstrate the specificity and veracity of this staining pattern. This antibody could not be used to examine DmATP7 expression in larval stages because it detects a nonspecific product not present in embryos.

DmATP7 *Is Essential for Early Larval Growth and Survival*

To determine the in vivo requirement for *DmATP7* function in *Drosophila*, imprecise P-element excision was used to generate a genomic deletion extending 798 base pairs into the *DmATP7* coding sequence from the start codon. To confirm that this deletion was a loss-of-function allele, male *DmATP7* $^{-}$*/Y* embryos (distinguished from their female *DmATP7* $^{+/+}$ and *DmATP7* $^{+/-}$ siblings using a GFP balancer chromosome) were probed with the anti-MNK antibody. Compared with their wild-type siblings, *DmATP7* $^{-}$*/Y* embryos did not show any signal, confirming that no detectable *DmATP7* protein is produced from the disrupted locus (Figure 2A).

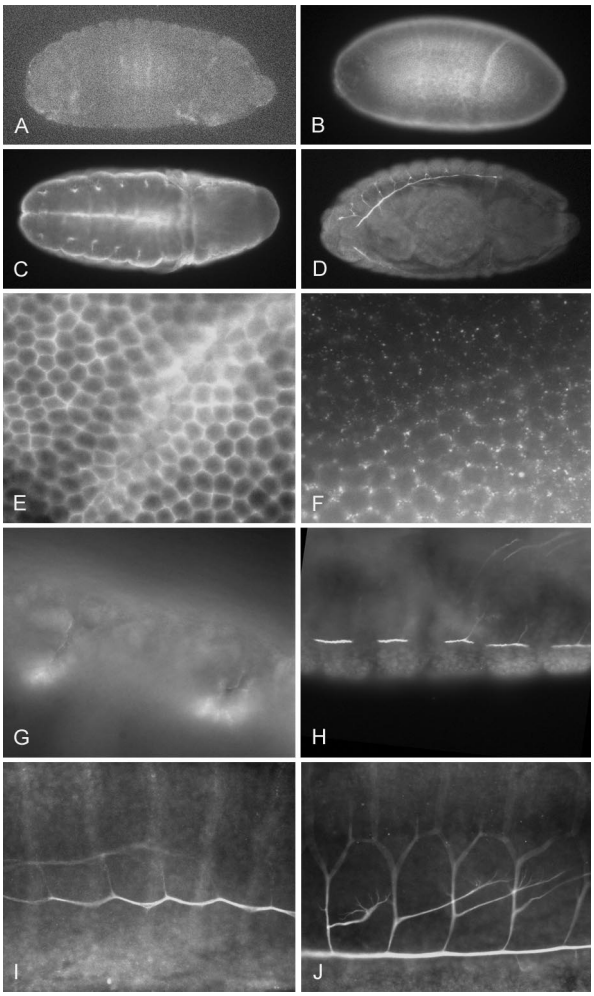

Figure 2. Mutant and wild-type embryos stained with anti-MNK antibody. (A) *DmATP7* $^{-}$*/Y* embryos show no staining with anti-MNK antibody. (B and E) Membranal staining is observed at 0–2 h AEL, becoming punctate by 4 h AEL (F). Staining is visible in the early tracheal placodes (C and G) from 4 h and remains visible in the developing tracheal dorsal trunk (H and I) and in branching trachea (D and J). Original magnification, 40× (A–D), 1000× (E–G), and 400× (H–J).

DmATP7 $^{-}$*/Y* animals were examined for any defects arising from disruption of *DmATP7* (Figure 3). Although at hatching there is no size difference between *DmATP7* $^{-}$*/Y* larvae and heterozygous/wild-type siblings, the mutant animals seem extremely lethargic in comparison with their wild-type siblings (see video in Supplemental Material 2), and their mouthparts are smaller and reduced in pigmentation (compare Figure 3, E and F). Unlike heterozygous and wild-type animals, *DmATP7* $^{-}$*/Y* larvae fail to grow and develop to the second instar (Figures 3, A–D), dying by 36 h after hatching. This lethality can be rescued by a full-length *DmATP7* transgene (discussed below), which restores mouthpart size and pigmentation (Figure 3G), normal growth, and activity (see video in Supplemental Material 2), resulting in viable adults that are slightly lacking in cuticle pigment, indicating the phenotypes observed are solely the result of *DmATP7* disruption.

To determine whether *DmATP7* $^{-}$*/Y* larvae are dying from excess or insufficient copper, rescue experiments with copper-depleted and copper-supplemented media were attempted. *DmATP7* $^{-}$*/Y* larvae die at the same stage on all types of media tested. To exclude the trivial possibility that mutant larvae were dying simply because they could not feed, medium containing food-dye was used to show that *DmATP7* $^{-}$*/Y* larvae do feed, although considerably less than their wild-type siblings (our unpublished data).

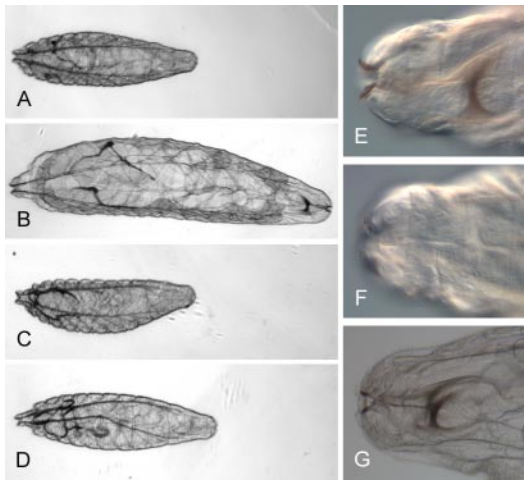

Figure 3. (A and B) Wild-type larvae <2 h after hatching (A) and 24 h after hatching (B). (C and D) *DmATP7* $^{-}$*/Y* larvae <2 h after hatching (C) and 24 h after hatching (D). *DmATP7* $^{-}$*/Y* larvae do not show significant growth in 24 h on normal media. (E and F) Mouth hooks of the larva shown in B (E) and the larva shown in D (F). *DmATP7* $^{-}$*/Y* mouth hooks lack normal pigmentation. (G) Mouth hooks of a *DmATP7* $^{-}$*/Y* larvae containing a *UAS-DmATP7* transgene that rescues the mutant animals to adulthood—mouth hook pigmentation and structure are restored. These larvae are siblings developing on the same media. Original magnification, 40× (A–D) and 400× (E–G).

Copper Is Likely to Accumulate in the Gut of DmATP7 Mutant Larvae

Direct detection of copper levels in first instars is technically difficult due to their small size, ~1/100th the mass of third instars. Copper levels from 500 wild-type first instars were barely detectable by inductively coupled plasma mass spectrometry. Furthermore, we were unable to detect any activity of the copper-dependent enzyme tyrosinase in up to 2000 wild-type first instars, whereas five wild-type third instars showed considerable tyrosinase activity. Due to these technical constraints, we sought to use transcript levels of the copper-responsive genes *Ctr1B* and *MtnA*, *B*, *C*, and *D* as proxy markers of copper accumulation in wild-type and mutant animals. *Ctr1B*, one of the three *Drosophila* copper uptake genes, is up-regulated in response to copper starvation (Zhou *et al*., 2003; Selvaraj *et al*., 2005), whereas all four *Drosophila metallothionein* genes (*MtnA–D*) are known to be up-regulated in high copper conditions (Lastowski-Perry *et al*., 1985; Mokdad *et al*., 1987; Egli *et al*., 2003). First, gut (the primary uptake organ) and fat bodies (the key detoxification organ of the insect, with functional similarities to the mammalian liver; Sondergaard, 1993) were dissected from wild-type third instars and analyzed for transcript levels (Table 2A). Strong up-regulation of *MtnA–D* was observed in the gut and fat body tissues of larvae fed a copper-supplemented diet. Up-regulation of *Ctr1B* in response to copper starvation and down-regulation in response to copper (previously demonstrated only in whole larvae) was predominant in gut tissues but also observed in fat bodies.

Table 2. Gene expression

	Ctr1A	Ctr1B	MtnA	MtnB	MtnC	MtnD
A. Gene expression in gut and fat bodies of wild-type third instars (relative to respective NF data points)						
Fat body BCS	1.29 ± 0.25	1.57 ± 0.13[a]	1.26 ± 0.41	1.08 ± 0.30	1.62 ± 0.27	0.96 ± 0.14
Fat body NF	1.00 ± 0.06	1.00 ± 0.05	1.00 ± 0.09	1.00 ± 0.06	1.00 ± 0.11	1.00 ± 0.14
Fat body Cu	1.30 ± 0.36	0.47 ± 0.13[a]	3.86 ± 0.78[a]	9.50 ± 3.52	12.8 ± 3.10[a]	6.10 ± 2.02
Gut BCS	0.78 ± 0.13	5.14 ± 1.29[b]	0.49 ± 0.09[b]	0.78 ± 0.12	0.87 ± 0.11	0.39 ± 0.06[b]
Gut NF	1.00 ± 0.06	1.00 ± 0.11	1.00 ± 0.13	1.00 ± 0.06	1.00 ± 0.05	1.00 ± 0.10
Gut Cu	1.05 ± 0.14	0.22 ± 0.04[b]	4.45 ± 0.41[b]	23.8 ± 5.30[b]	29.3 ± 5.60[b]	3.95 ± 0.64[b]
B. Gene expression (relative to WT NF) in wild-type and *DmATP7*$^{-}$*/Y* first instars						
WT BCS	3.17 ± 0.37[c]	9.94 ± 1.95[c]	0.59 ± 0.15[c]	0.70 ± 0.17	0.74 ± 0.08	0.56 ± 0.01[c]
WT NF	1.00 ± 0.06	1.00 ± 0.14	1.00 ± 0.08	1.00 ± 0.41	1.00 ± 0.38	1.00 ± 0.19
WT Cu	2.06 ± 0.39	1.24 ± 0.06	8.67 ± 1.04	39.7 ± 14.0	111 ± 55.5	21.3 ± 3.88
DmATP7^{-} *BCS*	0.46 ± 0.12[d]	0.50 ± 0.10[d]	0.50 ± 0.16	0.66 ± 0.34	0.21 ± 0.12[d]	0.46 ± 0.08
DmATP7^{-} *NF*	0.51 ± 0.08[c]	0.76 ± 0.21	0.79 ± 0.14	0.75 ± 0.38	1.38 ± 0.78	0.43 ± 0.02[c]
DmATP7^{-} *Cu*	0.52 ± 0.12	0.55 ± 0.10[e]	5.21 ± 2.28	6.11 ± 3.21[e]	11.3 ± 6.19	1.84 ± 0.37[e,f]

(A) Values from fat bodies and gut tissues are expressed relative to the same tissue exposed to normal food media (NF) and are the mean ± SEM of eight replicates from two independent experiments. Gene expression was normally distributed and a one-sample *t* test was used to determine significant differences. (B) Values are expressed relative to control larvae exposed to normal food and are the mean ± SEM of four replicates from two independent experiments. *Ctr1A* expression was normally distributed, and a one-way ANOVA with Games–Howell post hoc test was used to determine significant differences. *Ctr1B*, *MtnA*, *MtnB*, *MtnC*, and *MtnD* expression levels were not normally distributed and a Mann–Whitney test was used to determine significant differences.

[a] $p < 0.05$ compared with fat bodies exposed to normal food.

[b] $p < 0.05$ compared with gut tissue exposed to normal food.

[c] $p < 0.05$ compared with control flies exposed to normal food.

[d] $p < 0.05$ compared with control larvae exposed to copper-deficient media.

[e] $p < 0.05$ compared with control flies exposed to copper-supplemented media.

[f] $p < 0.05$ compared with *DmATP7* $^{-}$*/Y* flies exposed to normal food.

Because *DmATP7* $^{-}$*/Y* larvae do not survive until third instar, and first instars are too small to dissect, transcript levels were compared between whole knockout and wild-type first instars (Table 2B). Like dissected third instars, wild-type first instars showed up-regulation of *MtnA–D* in response to high copper and up-regulation of *Ctr1B* in response to copper starvation. *MtnA–D* gene expression also increased in *DmATP7* $^{-}$*/Y* larvae in response to a high copper diet, indicating copper is taken up at least into the gut. Importantly, no up-regulation of *Ctr1B* was seen in response to copper starvation in the mutant larvae. Up-regulation of *Ctr1B* is presumably a response to low copper levels in the gut cells (where strong *Ctr1B* up-regulation was observed in third instars) where an increase in the amount of uptake protein would optimize copper absorption from copper-deficient food. The fact that no up-regulation is observed in *DmATP7* $^{-}$*/Y* larvae suggests that, even under copper-limiting conditions, sufficient copper levels are present in the gut cells of these larvae to avoid the starvation response. This situation is analogous to that of human Menkes disease patients, where copper can be taken up into gut cells (inducing *Mtn* up-regulation) but remains trapped in these cells (thus no *Ctr1B* up-regulation) and cannot be transported to other tissues of the body.

To confirm that the changes in gene regulation we had quantified in first instars by reverse transcription-PCR were indeed confined predominantly to the gut region, we monitored expression of two enhanced yellow fluorescent protein (EYFP) fusion constructs, one under the control of the *MtnA* 5′ regulatory region, and the other under the control of the *Ctr1B* 5′ regulatory region (Figure 4). These results clearly show that *MtnA* and *Ctr1B* expression is confined almost exclusively to the gut region in first instar and that *DmATP7* $^{-}$*/Y* mutant larvae do respond to high copper exposure (*MtnA-EYFP* up-regulation) but do not respond to copper starvation (*Ctr1B-EYFP* up-regulation), supporting our argument that in the mutant animals, copper is taken into the gut cells but is retained there and is unable to reach the rest of the animal, resulting in lethality.

Expression Pattern of a DmATP7 *Rescue Transgene Supports Copper Uptake Role in the Gut*

In the course of overexpression experiments described later, a *UAS-DmATP7* transgene was found to serendipitously rescue *DmATP7* $^{-}$*/Y* animals to adulthood in the absence of a GAL4 driver, indicating that the transgene had inserted near an endogenous enhancer that drives sufficient *DmATP7* expression for survival. Attempts to rescue *DmATP7* $^{-}$*/Y* animals with numerous constitutive, gut, and fat body-specific GAL4 drivers all failed, indicating a very specific *DmATP7* expression pattern is required for survival. The expression pattern of the rescuing *UAS-DmATP7* transgene was investigated in third instars by immunostaining using the FLAG-epitope tag attached to the transgenic DmATP7, providing some evidence of the tissue-specific requirements for *DmATP7* (Figure 5). Low level cytoplasmic DmATP7-FLAG expression was observed in the imaginal discs, whereas strong nuclear/cytoplasmic staining was seen in discrete sections of the gut, including the foregut and hindgut imaginal rings, the large acid-secreting "copper cells" (Dubreuil, 2004) of the middle midgut, (Figure 5, A and D), the posterior midgut adjoining the hindgut (Figure 5, C and F), and all of the hindgut. The strong expression of this rescuing transgene in the midgut is consistent with a significant role for *DmATP7* in copper absorption from the diet, but a *DmATP7* regulatory region reporter construct is needed to make any definitive statements regarding the tissue-specific requirements of *DmATP7*.

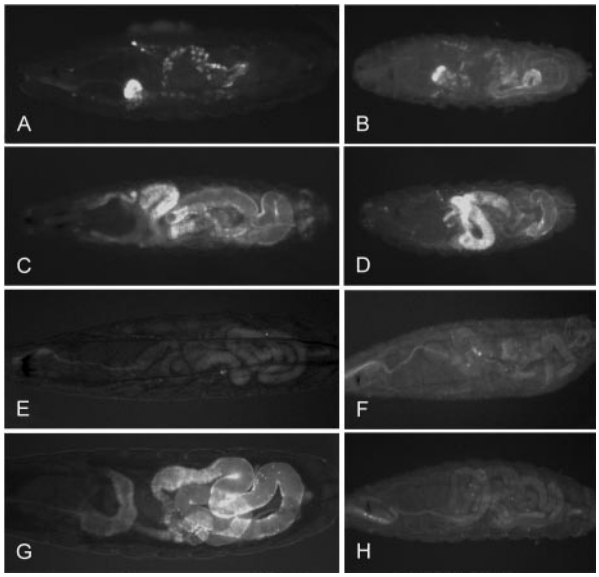

Figure 4. (A–D) Expression of *MtnA5′-EYFP* in wild-type (A and C) and *DmATP7* $^{-}$*/Y* (B and D) first instars raised for 6 h on normal food (A and B) or 1 mM copper food (C and D). Basal *MtnA5′-EYFP* expression is higher in mutant larvae, but both wild-type and mutant larvae respond robustly to a high copper diet. (E–H) Expression of *Ctr1B5′-EYFP* in wild-type (E and G) and *DmATP7* $^{-}$*/Y* (F and H) first instars raised for 12 h on 1 mM copper food (E and F) or 100 μM BCS food (G and H). Only wild-type larvae respond to copper starvation on BCS food by up-regulation of *Ctr1B5′-EYFP*.

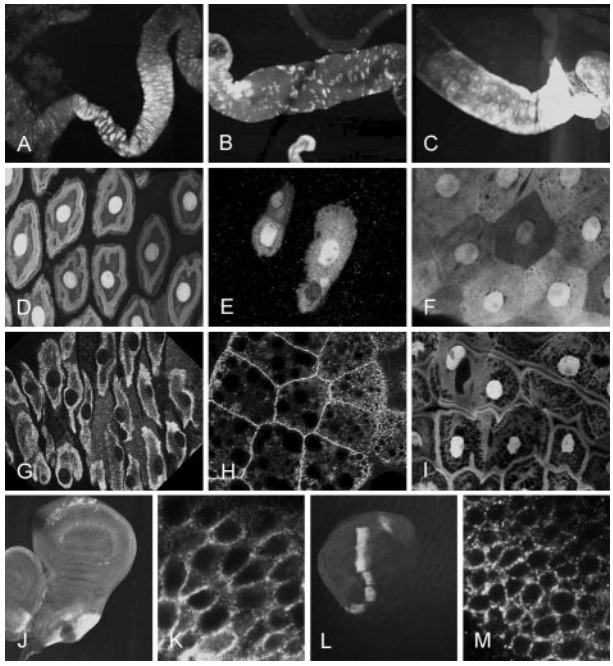

Figure 5. (A–F, and J) Expression of transgenic DmATP7^{wt}-FLAG in rescued *DmATP7* $^{-}$*/Y; UAS-DmATP7*^{wt}*-FLAG* third instars. All shown anterior to left. (A–F) DmATP7^{wt}-FLAG expression in middle midgut (A, B, D, and E) and posterior midgut (C and F). In all cases, DmATP7^{wt}-FLAG is observed in both the nuclei and the cytoplasm of these gut cells. (G) DmATP7^{wt}-FLAG in middle midgut cells under a strong gut enhancer GAL4 control; expression is excluded from the nucleus in this case. (H) Ectopic DmATP7^{wt}-FLAG in fat body cells; clear PM localization is observed. (I) DmATP7^{wt}-FLAG expression in posterior midgut of larvae exposed to high copper diet; occasional relocalization to PM is observed compared with F. (J) Expression of DmATP7^{wt}-FLAG under *Pnr-GAL4* control in the *Pnr* domain of the third instar wing imaginal disk. (K) High-magnification view of J; strong staining is observed in a punctate pattern localized or proximal to the PM. (L) Expression of DmATP7^{wt}-FLAG under *Ptc-GAL4* control in the *Ptc* domain of the third instar wing imaginal disk. (M) High-magnification view of L; strong staining is observed in a punctate pattern localized to the PM. When either DmATP7^{tap}-FLAG, DmATP7^{mbs}-FLAG, or DmATP7^{cpc}-FLAG expression is driven by *Pnr-GAL4* or *Ptc-GAL4*, localization of the mutant protein is the same as that seen for the wild-type overexpressed protein (our unpublished data). Original magnification, 100× (A-C, J, and L) and 630× (D–J, K, and M).

Unlike the mammalian MNK protein that clearly translocates from the TGN to the PM upon copper stimulation in certain cultured mammalian cells, PM staining of DmATP7-FLAG was only very rarely seen in larvae fed a copper-supplemented diet (compare Figure 5, I with F) and never in larvae fed a normal or copper-deficient diet. However, when overexpressed under GAL4 control, DmATP7-FLAG staining is excluded from the nucleus (Figure 5G), and overexpression also causes clear DmATP7-FLAG staining in the PM of fat body cells (Figure 5H). Therefore, under artificially high expression levels DmATP7 can localize to the PM, suggesting it contains appropriate PM trafficking/retention information (putative trafficking motifs are outlined in Figure 1). Generation of a DmATP7-specific antibody is required to further investigate the localization of the endogenous protein in these key tissues and to avoid artifacts caused by overexpression.

There Is a Significant Maternal Contribution of DmATP7

Germline clone-derived embryos devoid of maternal *DmATP7* product were examined to investigate the degree of maternal contribution from the *DmATP7* locus. Despite the finding that DmATP7 is strongly expressed in embryonic tracheae (Figure 2), tracheal development in these embryos seems normal (Figure 6), suggesting this expression may reflect a functional rather than a structural role for *DmATP7* in the tracheae. These mutant embryos, although alive and apparently fully developed, are unable to hatch. This more extreme phenotype reveals a significant maternal contribution that is required for hatching but not for oogenesis. Because *DmATP7* $^{-}$*/Y* larvae have hypopigmented mouth hooks (Figure 3), the more extreme maternal phenotype could be due to weak mouth hooks unable to penetrate the chorion and facilitate hatching. This phenotype is not affected by raising parents on either copper-deficient or copper-supplemented media (our unpublished data). This is the first evidence of such an early requirement for correct copper homeostasis in *Drosophila* and demonstrates a striking requirement for *DmATP7* before feeding has commenced, for essential processes in addition to absorption of copper via the gut.

DmATP7 Is Required for Adult Cuticle Pigmentation

In mammals, the MNK protein is thought to supply copper to the pigment-forming enzyme tyrosinase (Petris *et al*., 2000), and mammals with reduced MNK function display hypopigmented hair/fur (Menkes *et al*., 1962; Hamza *et al*., 2001). Similarly, copper deficiency as a result of reduced *Ctr1B* copper uptake activity results in hypopigmented cuticle in *Drosophila* (Zhou *et al*., 2003). Because *DmATP7* $^{-}$*/Y* mutants die early in larval development, heterozygous

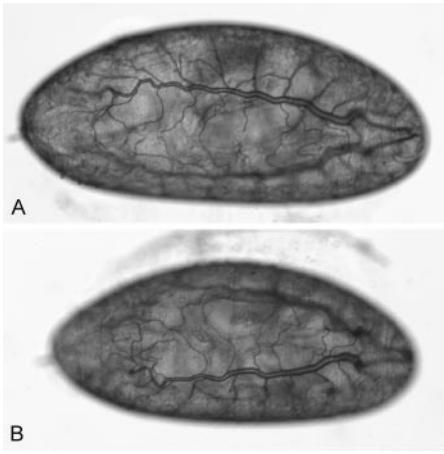

Figure 6. Wild-type embryo (A) and *DmATP7* $^{-/-}$ germline cloned-derived embryo (B) devoid of maternal *DmATP7* at 50× magnification. Mutant embryos have visibly normal tracheal development, despite the absence of DmATP7 expression in this tissue. No other developmental defects are visible, but the larvae fail to hatch.

adults containing *DmATP7* $^{-/-}$ clones were generated using the flippase-FRT system (Xu and Rubin, 1993) to examine any role of *DmATP7* in pigment formation. Patches of depigmented tissue were observed in the thorax (Figure 7) and abdomen (our unpublished data), but no morphological defects were observed, indicating that *DmATP7*, like *MNK* in mammals, is essential for adult pigment formation.

Overexpression of Wild-Type DmATP7

To examine the effects of increased expression of a copper-transporting P-type ATPase in a multicellular organism, the GAL4-UAS system was used to drive expression of wild-type or mutant *UAS-DmATP7* transgenes in a tissue-specific manner in *Drosophila*.

Overexpression of DmATP7 Results in Hypopigmentation

Unexpectedly, ubiquitous overexpression of *DmATP7* resulted in dramatic hypopigmentation of the abdomen of animals grown on copper-deficient medium (Figure 8, A and B), a phenotype previously observed in copper-starved *Ctr1B* $^{+/-}$ flies (Zhou *et al*., 2003), whereas darker pigmentation was observed on the head cuticle of these flies. Add-

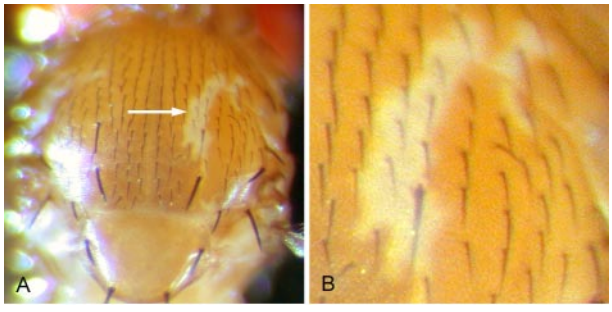

Figure 7. An example of a *DmATP7* $^{-/-}$ clone in the adult *Drosophila* thorax at 500× (A) and 1000× (B) magnification. Although the clones have no cuticular markers, the depigmentation phenotype seen is not observed in control clones (our unpublished data), indicating it is due to *DmATP7* $^{-/-}$ tissue.

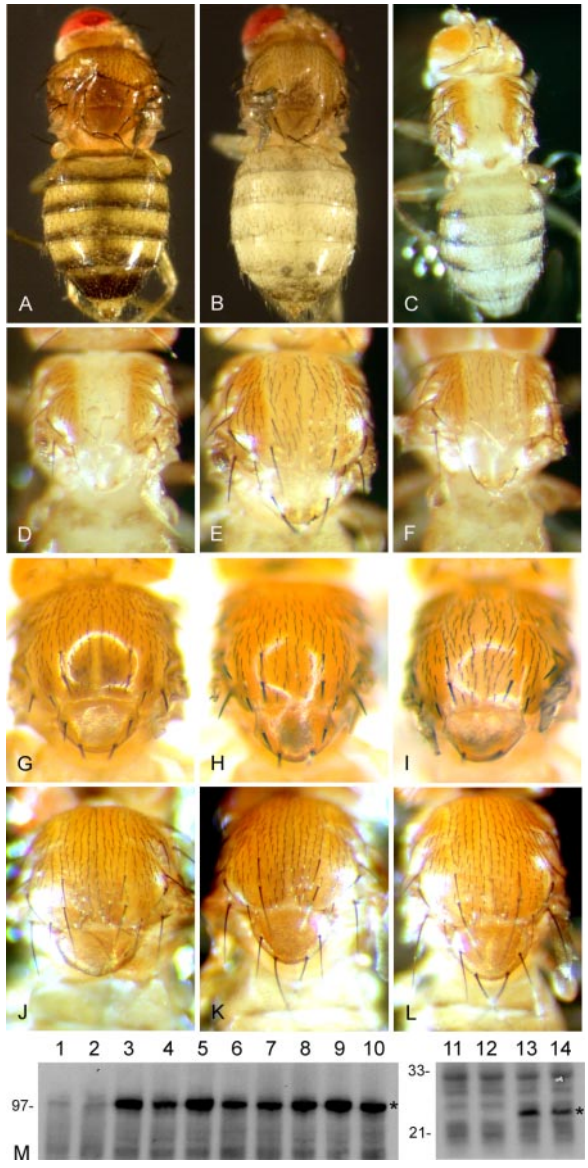

Figure 8. (A and B) *Act-GAL4/UAS-DmATP7*^{wt} flies grown on normal medium (A) and 10 mM TTM medium (B). In the *DmATP7*-overexpressing flies grown on copper-deficient media (B), reduction in pigmentation is seen throughout the adult abdominal cuticle, whereas increased pigmentation is observed in the head cuticle. Full-length (C) and close-up views (D) of *Pnr-GAL4/UAS-DmATP7*^{wt} adults. Overexpression of *DmATP7*^{wt} causes strong hypopigmentation in the *Pnr* expression domain of the thorax and abdomen and loss of thoracic bristles, reduction of the scutellum, and a cleft in the thorax. In contrast, overexpression of *DmATP7*^{mbs} (E) and *DmATP7*^{cpc} (F) under the same GAL4 driver causes hypopigmentation in the thorax and abdomen (albeit milder in the abdomen), but only mild loss of thoracic bristles, and mild or no thoracic cleft/scutellar reduction. (G) Expression of *Ctr1A* under *Pnr-GAL4* control has no phenotypic effect. Coexpression of *Ctr1A* rescues the *DmATP7*^{wt} overexpression phenotype (H) but not the *DmATP7*^{cpc} overexpression phenotype (I). (J–L) Expression of *DmATP7*^{wt} (J) under *Ptc-GAL4* control causes reduction in the scutellum and loss of the major scutellar bristles, whereas expression of *DmATP7*^{tap} (K) and *DmATP7*^{mbs} (L) with the same GAL4 driver has no phenotypic effect. (M) Anti-FLAG Western blot showing expression in adult heads under GMR-GAL4 control of negative controls (1, 2, 11, and 12), *DmATP7*^{wt} (3 and 4), *DmATP7*^{cpc} (5 and 6), *DmATP7*^{tap} (7 and 8), *DmATP7*^{mbs} (9 and 10), and *Ctr1A* (13 and 14). Two independent insertion lines for each transgene are shown. Asterisk (*) shows DmATP7 and Ctr1A bands.

back experiments supplementing this medium with copper, zinc, or iron showed that the phenotype is due specifically to lack of copper (Table 1). Thus, overexpression of *DmATP7* seems to be creating a functional copper deficiency in certain cuticular cells, phenocopying the effect of loss of *DmATP7* expression. When *UAS-DmATP7* expression was driven under control of the *Pannier (Pnr)-GAL4* driver, dramatic hypopigmentation was observed only in the *Pnr* expression domain, a strip of cuticular cells down the center of the adult thorax and abdomen (Figure 8C). A strong cleft in the thorax, reduction of the scutellum, and loss of thoracic bristles (Figure 8, C and D) was also observed. Unlike the *Act-GAL4/UAS-DmATP7* hypopigmentation, the *Pnr-GAL4/UAS-DmATP7* hypopigmentation is independent of dietary copper levels, indicating a more extreme functional copper deficiency.

The *Pnr-GAL4/UAS-DmATP7* hypopigmentation phenotype is almost completely rescued by simultaneous overexpression of the copper uptake gene *Ctr1A* (Figure 8H) but not by cooverexpression of either *DmAtox1* or *DmCCS* (*Drosophila* orthologues of the mammalian *Atox1* and *CCS* copper chaperone genes; Southon *et al*., 2004), suggesting it is the result of a copper deficiency caused by increased efflux and that copper balance is restored by increasing the rate of copper uptake. Overexpression of *Ctr1A*, *DmAtox1*, or *DmCCS* alone has no effect on pigmentation (Figure 8G; our unpublished data). Although the hypopigmentation caused by *DmATP7* overexpression in cuticular cells is suggestive of increased copper efflux from these cells, we wanted to further explore this phenotype by generating *UAS-DmATP7* transgenes with mutations in key catalytic residues. According to in vitro studies with mammalian, yeast and bacterial P-type ATPases, ablation of the DKTG transient acyl phosphorylation site (TAP; Figure 1) or the transmembrane CPC motif (CPC; Figure 1) should render DmATP7 catalytically inactive, unable to transport copper across membranes, and therefore unable to export copper from the cell (Forbes and Cox, 1998; Voskoboinik *et al*., 2001). Ablation of the metal binding sites (MBS; Figure 1) should have the same effect under copper limiting conditions and compromise activity under normal conditions (Lutsenko and Petris, 2002; Voskoboinik and Camakaris, 2002).

Surprisingly, expression of the three mutated forms of *DmATP7* under *Pnr-GAL4* control still resulted in dramatic hypopigmentation, although the morphological defects caused by wild-type *DmATP7* overexpression were reduced or absent (Figure 8, E and F). Importantly, however, coexpression of *DmCtr1A* fails to rescue the hypopigmentation caused by these mutated forms of *DmATP7* (Figure 8I) despite their less severe phenotype, indicating that separate mechanisms are causing the hypopigmentation phenotype in the wild-type and mutant cases. Under control of the *Patched (Ptc)-GAL4* driver, expression of wild-type *DmATP7* resulted in a reduction of the scutellum and partial or complete loss of the scutellar bristles (Figure 8J), whereas expression of the inactive mutants had no effect (Figure 8, K and L), reinforcing the differing activities of these transgenes. Similarly, overexpression of wild-type *DmATP7* in the tracheae resulted in late larval/early pupal death (our unpublished data), a phenotype not caused by catalytically inactive *DmATP7*. At least three independent insertion lines were tested for each transgene to rule out possible insertion effects, and expression levels for two insertion lines of each construct are shown by Western blot (Figure 8M) to demonstrate that the mutations introduced are not affecting protein stability.

The subcellular localization of the overexpressed DmATP7 forms was examined to determine whether this might explain the differences in the observed phenotypes. Predominantly PM staining was observed with all four transgenes when expressed in the wing imaginal disk either under *Pnr-GAL4* or *Ptc-GAL4* control (Figure 5, J–M). This staining is in stark contrast to the cytoplasmic staining observed in imaginal discs and gut cells of *DmATP7* $^{-}$*/Y* larvae rescued by low levels of transgene-derived *DmATP7* expression (Figure 5, A–I), suggesting that high levels of expression of the DmATP7 protein result in a partial shift in subcellular localization, and this shift could be responsible for the overexpression phenotype.

DISCUSSION

Recently, the power of *Drosophila* genetics has been bought to bear on the investigation of copper homeostasis in a highly productive manner (Egli *et al*., 2003; Zhou *et al*., 2003; Southon *et al*., 2004). The metal-responsive transcription factor MTF-1 has been shown to be necessary in *Drosophila* for response to both excess and copper-limiting conditions, with *MTF-1* mutants dying on high copper load and undergoing developmental arrest in copper-limiting conditions (Egli *et al*., 2003). It has subsequently been shown that a mutation in one of the three *Drosophila* copper import genes, *Ctr1B*, also causes sensitivity to both copper deficiency and copper load. *Ctr1B* mutants undergo developmental arrest and death at early second instar when grown in copper-limiting conditions, and die at late pupal stages when raised under high copper conditions (Zhou *et al*., 2003).

The current study presents data on the role of the third key component of *Drosophila* copper homeostasis, the sole *Drosophila* orthologue of the mammalian MNK and WND copper-transporting P-type ATPases. We have previously described a requirement for *DmATP7* in copper efflux from cultured *Drosophila* embryonic S2 cells (Southon *et al*., 2004). This study demonstrates conservation of function between *DmATP7* and its mammalian orthologues and shows that *DmATP7* function is absolutely required in vivo for completion of embryogenesis, early larval growth and development, and adult pigmentation of the insect. Strikingly, unlike *Ctr1B* and *MTF-1*, the early embryonic requirement for *DmATP7* is independent of dietary copper levels and is observed even before feeding stages.

Copper-dependent phenol oxidases such as tyrosinase are involved in the production of biogenic amines needed for cuticle sclerotization and pigmentation, neurotransmitter production, and protein and chitin cross-linking at eclosion and molting (Wright, 1987). The range of *DmATP7* mutant phenotypes described here correlates well with disruption to all of these pathways. First, disruption of endogenous *DmATP7* activity bleaches both *yellow*$^{+}$ and *yellow*$^{-}$ cuticle, indicating that *DmATP7* activity is required for production of all three pigment components, Dopa melanin, dopamine melanin, and NBAD sclerotin, in agreement with the proposed requirement of copper for phenol oxidase activity (Wright, 1987). Second, the majority of mutations in the genes encoding two central components of the pigmentation pathway, Dopa decarboxylase (*Ddc*) and tyrosine hydroxylase (*pale*), result in active larvae that are unable to eclose and have hypopigmented mouthparts (Jurgens *et al*., 1984), an identical phenotype to that seen in the *DmATP7* mutants lacking maternal contribution. Third, several alleles in the *Ddc* gene cluster result in thoracic and bristle defects similar to those seen in *DmATP7* overexpressing mutants (Wright, 1987).

Finally, the lethargic behavior of *DmATP7* $^{-}$*/Y* larvae could be explained by impaired neuronal function as a result of loss of copper-dependent *Ddc*-mediated neurotransmitter production or could reflect a role for DmATP7 similar to that of MNK in *N*-methyl-D-aspartate receptor-dependent neuronal activation (Schlief *et al*., 2005). Alternatively, the discovery of DmATP7 expression in developing tracheae suggests that lethargy could also be explained by a respiratory defect, a possibility supported by the lethal effect of DmATP7 overexpression when driven in the tracheae. Egli *et al*. (2003) postulate a role for copper in cellular respiration, because it is essential for cytochrome *c* oxidase function. A combination of improperly functioning tracheae and low cytochrome *c* oxidase activity as a result of functional copper deficiency would very likely cause lethargy and eventual lethality.

One unexpected outcome of this study was the similarity in *DmATP7* loss-of-function and overexpression phenotypes in the adult cuticle, with both situations resulting in the loss of pigmentation. By analogy to MNK in mammalian cells, endogenous DmATP7 may normally reside in the TGN, with a fraction cycling constitutively between the TGN and the PM (Petris *et al*., 1996). We postulate that overexpressed DmATP7 might also accumulate at the PM, as previously seen for MNK in mammalian cells (Greenough and Camakaris, personal communication), where it would constitutively pump copper from the cell, resulting in a depletion of cellular copper levels. Indeed we have observed both wild-type and mutant DmATP7-FLAG localized to the PM. Copper levels can be restored by increasing copper uptake with *Ctr1A* overexpression, as we have observed. Catalytically inactive DmATP7 causes a similar but less severe phenotype. We postulate that this is a dominant negative effect whereby some of the overexpressed mutant DmATP7 is displacing endogenous wild-type DmATP7 from its TGN docking sites. The inactive DmATP7 cannot however transport copper into secretory pathway, thus depriving tyrosinase of its essential cofactor. In this scenario, increasing copper uptake would have no affect on tyrosinase activity, because the mutant DmATP7 would still be displacing endogenous DmATP7 at the TGN. This is consistent with our observations that *Ctr1A* coexpression only rescues wild-type *DmATP7* overexpression.

A key characteristic of the MNK and WND proteins is their ability to undergo copper-stimulated trafficking from the TGN to the PM or cytoplasmic vesicles (Petris *et al*., 1996). We have been unable to demonstrate definitively that DmATP7 undergoes similar trafficking events. We have, however, observed both cytoplasmic and PM localization of endogenous DmATP7 in the embryo, compatible with the ability of DmATP7 to traffic. In addition, increased expression of transgene-derived DmATP7 results in a shift in localization from the cytoplasm to the PM, further demonstrating that DmATP7 contains PM localization signals. Resolution of this issue will require a DmATP7-specific antibody or live imaging with a GFP-DmATP7 fusion protein.

Using the genetic tools developed here, we can now start to decipher the complex transcriptional and posttranslational regulatory mechanisms required to maintain copper homeostasis in *Drosophila*, establishing a model for how multicellular organisms deal with metals that are both toxic and essential.

ACKNOWLEDGMENTS

We are grateful to Walter Schaffner, Ernst Hafen, and Paul Whitington for the gifts of fly stocks. We also thank Len Kelly for comments on the manuscript. This work was supported financially by the International Copper Association, the Australian Research Council through its Special Research Centre and Discovery Grants programs, and through a grant from the University of Melbourne Research Grants Scheme. R. B. was a recipient of a Peter Doherty Fellowship from the National Health and Medical Research Council and the J. N. Peters Bequest Fellowship from the University of Melbourne.

REFERENCES

Camakaris, J., Petris, M. J., Bailey, L., Shen, P., Lockhart, P., Glover, T. W., Barcroft, C., Patton, J., and Mercer, J. F. (1995). Gene amplification of the Menkes (MNK; ATP7A) P-type ATPase gene of CHO cells is associated with copper resistance and enhanced copper efflux. Hum. Mol. Genet. *4*, 2117–2123.

Danks, D. M. (1988). Copper deficiency in humans. Annu. Rev. Nutr. *8*, 235–257.

Danks, D. M. (1995). Disorders of copper transport. In: The Metabolic and Molecular Basis of Inherited Disease, ed. C. R. Scriver, A. L. Beaudet, W. M. Sly, and D. Valle, New York: McGraw-Hill, 2211–2235.

Danks, D. M., Campbell, P. E., Stevens, B. J., Mayne, V., and Cartwright, E. (1972). Menkes's kinky hair syndrome. An inherited defect in copper absorption with widespread effects. Pediatrics *50*, 188–201.

Dubreuil, R. R. (2004). Copper cells and stomach acid secretion in the *Drosophila* midgut. Int. J. Biochem. Cell Biol. *36*, 745–752.

Egli, D., Selvaraj, A., Yepiskoposyan, H., Zhang, B., Hafen, E., Georgiev, O., and Schaffner, W. (2003). Knockout of 'metal-responsive transcription factor' MTF-1 in *Drosophila* by homologous recombination reveals its central role in heavy metal homeostasis. EMBO J. *22*, 100–108.

Felsenstein, J. (1989). PHYLIP –phylogeny inference package (version 3.2). Cladistics *5*, 164–166.

Forbes, J. R., and Cox, D. W. (1998). Functional characterization of missense mutations in ATP7B: Wilson disease mutation or normal variant? Am. J. Hum. Genet. *63*, 1663–1674.

Halliwell, B., and Gutteridge, J. M. (1984). Oxygen toxicity, oxygen radicals, transition metals and disease. Biochem. J. *219*, 1–14.

Hamza, I., Faisst, A., Prohaska, J., Chen, J., Gruss, P., and Gitlin, J. D. (2001). The metallochaperone Atox1 plays a critical role in perinatal copper homeostasis. Proc. Natl. Acad. Sci. USA *98*, 6848–6852.

Jurgens, G., Wieschaus, E., Nusslein-Volhard, C., and Kluding, H. (1984). Mutations affecting the pattern of larval cuticle in *Drosophila melanogaster*. II. Zygotic loci on the third chromosome. Wilhelm Roux's Arch. Dev. Biol. *193*, 283–295.

Lastowski-Perry, D., Otto, E., and Maroni, G. (1985). Nucleotide sequence and expression of a *Drosophila* metallothionein. J. Biol. Chem. *260*, 1527–1530.

Lutsenko, S., and Petris, M. J. (2002). Function and regulation of the mammalian copper-transporting ATPases: insights from biochemical and cell biological approaches. J. Membr. Biol. *191*, 1–12.

Menkes, J. H., Alter, M., Steigleder, G. K., Weakley, D. R., and Sung, J. H. (1962). A sex-linked recessive disorder with retardation of growth, peculiar hair, and focal cerebral and cerebellar degeneration. Pediatrics *29*, 764–779.

Mokdad, R., Debec, A., and Wegnez, M. (1987). Metallothionein genes in *Drosophila melanogaster* constitute a dual system. Proc. Natl. Acad. Sci. USA *84*, 2658–2662.

Pena, M.M.O., Lee, J., and Thiele, D. J. (1999). A delicate balance: homeostatic control of copper uptake and distribution. J. Nutr. *129*, 1251–1260.

Petris, M. J., Mercer, J. F., Culvenor, J. G., Lockhart, P., Gleeson, P. A., and Camakaris, J. (1996). Ligand-regulated transport of the Menkes copper P-type ATPase efflux pump from the Golgi apparatus to the plasma membrane: a novel mechanism of regulated trafficking. EMBO J. *15*, 6084–6095.

Petris, M. J., Strausak, D., and Mercer, J. F. (2000). The Menkes copper transporter is required for the activation of tyrosinase. Hum. Mol. Genet. *9*, 2845–2851.

Robertson, H. M., Preston, C. R., Phillis, R. W., Johnson-Schlitz, D. M., Benz, W. K., and Engels, W. R. (1988). A stable genomic source of P element transposase in *Drosophila melanogaster*. Genetics *118*, 461–470.

Roelofsen, H., Wolters, H., Van Luyn, M. J., Miura, N., Kuipers, F., and Vonk, R. J. (2000). Copper-induced apical trafficking of ATP7B in polarized hepatoma cells provides a mechanism for biliary copper excretion. Gastroenterology *119*, 782–793.

Rozen, S., and Skaletsky, H. (2000). Primer3 on the WWW for general users and for biologist programmers. Methods Mol. Biol. *132*, 365–386.

Scheinberg, I. H., and Sternlieb, I. (1984). Wilson's disease, Philadelphia: WB Saunders.

Schlief, M. L., Craig, A. M., and Gitlin, J. D. (2005). NMDA receptor activation mediates copper homeostasis in hippocampal neurons. J. Neurosci. *25*, 239–246.

Selvaraj, A., Balamurugan, K., Yepiskoposyan, H., Zhou, H., Egli, D., Georgiev, O., Thiele, D. J., and Schaffner, W. (2005). Metal-responsive transcription factor (MTF-1) handles both extremes, copper load and copper starvation, by activating different genes. Genes Dev. *19*, 891–896.

Sondergaard, L. (1993). Homology between the mammalian liver and the *Drosophila* fat body. Trends Genet. *9*, 193

Southon, A., Burke, R., Norgate, M., Batterham, P., and Camakaris, J. (2004). Copper homoeostasis in *Drosophila melanogaster* S2 cells. Biochem. J. *383*, 303–309.

The FlyBase Consortium. (2003). The FlyBase database of the *Drosophila* genome projects and community literature. Nucleic Acids Res. *31*, 172–175.

Voskoboinik, I., and Camakaris, J. (2002). Menkes copper-translocating P-type ATPase (ATP7A): biochemical and cell biology properties, and role in Menkes disease. J. Bioenerg. Biomembr. *34*, 363–371.

Voskoboinik, I., Mar, J., Strausak, D., and Camakaris, J. (2001). The regulation of catalytic activity of the Menkes copper-translocating P-type ATPase. Role of high affinity copper-binding sites. J. Biol. Chem. *276*, 28620–28627.

Wright, T. R. (1987). The genetics of biogenic amine metabolism, sclerotization, and melanization in *Drosophila melanogaster*. Adv. Genet. *24*, 127–222.

Xu, T., and Rubin, G. M. (1993). Analysis of genetic mosaics in developing and adult *Drosophila* tissues. Development *117*, 1223–1237.

Yamaguchi, Y., Heiny, M. E., Suzuki, M., and Gitlin, J. D. (1996). Biochemical characterization and intracellular localization of the Menkes disease protein. Proc. Natl. Acad. Sci. USA *93*, 14030–14035.

Zhou, H., Cadigan, K. M., and Thiele, D. J. (2003). A copper-regulated transporter required for copper acquisition, pigmentation, and specific stages of development in *Drosophila melanogaster*. J. Biol. Chem. *278*, 48210–48218.